DOI: 10.1002/cbic.200500180

Replacement of Isobutyl by Trifluoromethyl in Pepstatin A Selectively Affects Inhibition of Aspartic Proteinases

Christoph Binkert,*[a] Massimo Frigerio,[b] Andrew Jones,[a] Solange Meyer,[a] Cristina Pesenti,[b] Lars Prade,[a] Fiorenza Viani,[b] and Matteo Zanda*[b]

*Two bis-trifluoromethyl pepstatin A analogues, carboxylic acid **1** and its methyl ester **2**, have been synthesised in order to probe the properties and size of the trifluoromethyl (Tfm) group and compare it to the "bigger" isobutyl that is present in pepstatin A. The results demonstrate that Tfm can effectively replace the isobutyl chain as far as inhibitory activity against plasmepsin II (PM II), an aspartic proteinase from* Plasmodium falciparum*, is concerned. On the other hand, replacement of isobutyl by Tfm selectively affected activity against other aspartic proteinases tested. Two lines of evidence led to these conclusions. Firstly, compounds **1** and **2** retained single-digit nanomolar inhibitory activity against PM II, but were markedly less active against PM IV, cathepsin D and cathepsin E. Secondly, the X-ray crystal structures of the three complexes of PM II with **1**, **2** and pepstatin A were obtained at 2.8, 2.4 and 1.7 Å resolution, respectively. High overall similarity among the three complexes indicated that the central Tfm was well accommodated in the lipophilic S_1 pocket of PM II, where it was involved in tight hydrophobic contacts. The interaction of PM II with Phe111 appeared to be crucial. Comparison of the crystal structures presented here, with X-ray structures or structural models of PM IV and cathepsin D, allowed an interpretation of the inhibition profiles of pepstatin A and its Tfm variants against these three enzymes. Interactions of the P_1 side chain with amino acids that point into the S_1 pocket appear to be critical for inhibitory activity. In summary, Tfm can be used to replace an isobutyl group and can affect the selectivity profile of a compound. These findings have implications for the design of novel bioactive molecules and synthetic mimics of natural compounds.*

Introduction

Although fluorine is considered to be rather close in size to hydrogen, it is now generally accepted that trifluoromethyl (Tfm) is a much larger group than methyl.[1] Indeed, based on the Charton steric parameter,[2] the value for the methyl group is 0.52 Å, isopropyl is 0.76 Å, Tfm is 0.91 Å and isobutyl is 0.97 Å.[3] However, Tfm is rotationally symmetric around the axis of its C–C bond, like the methyl group, whereas the isopropyl and isobutyl groups do not feature such rotational symmetry. One can therefore argue that, in terms of "effective bulk", the isotropic Tfm group occupies a considerably smaller volume than the anisotropic isopropyl and isobutyl groups, lying halfway between an isopropyl and methyl group.[4] This study was undertaken in order to probe the properties of Tfm when used as a substitute for an isobutyl group in medicinal chemistry. This structural modification could have implications for the design of novel bioactive molecules and synthetic mimics of natural compounds.[5] Fluorine substitution is, in fact, a powerful tool in medicinal chemistry.[6] A number of reasons can be listed in favour of fluorine substitutions. Among these are the increased hydrolytic and metabolic stability that arise from the chemical inertness of the C–F bond, the sometimes increased hydrophobic nature of fluorinated functions and the possibility of achieving improved oral bioavailability of fluoroorganic compounds. Advantage can be taken of these potential benefits because fluorine and fluorinated functions have been reported to effectively replace critical functionalities in the parent molecule. For example, fluorine atoms have been used to replace hydrogen or hydroxy groups, or CF_2 has been used as a mimic for oxygen atoms. Further interest in this topic has been raised by the recent work by Diederich et al.,[7] who have studied the local-environmental features of several proteins in terms of fluorophilicity and fluorophobicity. This has paved the way for an innovative understanding of the peculiar properties of fluoroorganic substrates in medicinal chemistry and biology.[8]

Within the frame of a project aimed at studying the effects of fluoroalkyl incorporation in the backbone of peptidomimetic-proteinase inhibitors, we have recently described the total synthesis of a bis-Tfm analogue (**1**) of pepstatin A (Scheme 1)

[a] *Dr. C. Binkert, A. Jones, Dr. S. Meyer, Dr. L. Prade*
Actelion Pharmaceuticals Ltd.
Gewerbestrasse 16, 4123 Allschwil (Switzerland)
Fax: (+41) 61-487-4500
E-mail: christoph.binkert@actelion.com

[b] *M. Frigerio, Dr. C. Pesenti, Dr. F. Viani, Dr. M. Zanda*
C.N.R.—Istituto di Chimica del Riconoscimento Molecolare
Sezione "A. Quilico" and
Dipartimento di Chimica Materiali ed Ingegneria Chimica "G. Natta"
Politecnico di Milano, via Mancinelli 7, 20131 Milano (Italy)
Fax: (+39) 02-2399-2080
E-mail: matteo.zanda@polimi.it

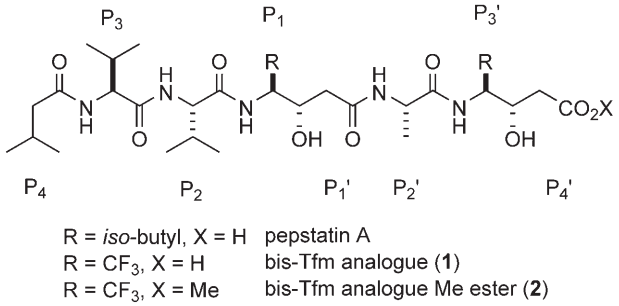

Scheme 1. Pepstatin A and its bis-trifluoromethyl analogues **1** and **2**.

in which both isobutyl statine side chains were replaced by Tfm groups.[9] Pepstatin A is a peptide-like natural compound, initially isolated from various species of *Streptomyces*.[10] Pepstatin A acts as a very potent, but relatively unspecific inhibitor of many aspartic proteinases. This class of enzymes includes, amongst others, the human proteins pepsin, renin, cathepsins D and E, as well as the protozoal plasmepsins (PMs).[11] PMII and PMIV have been shown to be located inside the food vacuole of *Plasmodium falciparum*, which is the agent responsible for the most severe form of malaria. These enzymes are believed to be involved in host-cell protein degradation, in particular haemoglobin—a process crucial to the survival of the parasite during the blood stage of its infectious cycle.[12] The suggestion of the concept that inhibition of plasmepsins has antimalarial effects is based on the observation that pepstatin A and small-molecular-weight plasmepsin inhibitors reduce *P. falciparum* proliferation in human red blood cells, in vitro.[13] Therefore, PMII and PMIV serve as drug targets for antimalarial therapies and well-characterised activity assays for these enzymes are available.[14]

Several analogues of pepstatin A have been reported in which the central isobutyl-statine residue in the P_1 region has been replaced by other lipophilic groups, such as benzyl.[15,16] Like pepstatin A, these compounds showed excellent inhibitory properties against PMII enzymatic activity in vitro, but they displayed weak antiparasitic activity in cell-culture assays and showed no significant improvement over pepstatin A.[17]

Here we report the results of the biological evaluation of pepstatin A variant **1**, its methyl ester **2** (Scheme 1) and several truncated peptidomimetics that incorporate Tfm-statine. We show that **1** and **2** are potent inhibitors of PMII and feature improved selectivity against PMIV and the human cathepsins D and E. We also describe the X-ray crystal structures of PMII complexed with either **1** or **2**. These are, to the best of our knowledge, the first X-ray structures available in the Protein Data Bank (PDB) of enzyme complexes with a ligand that bears a Tfm group in a purely aliphatic context, particularly as a peptidic-backbone substituent. The X-ray structures of PMII complexed to **1** or **2** are compared to PMII complexed to pepstatin A, which we describe here at a higher resolution than that currently available in the PDB.[15a] We present evidence from these structures that confirms that Tfm acts as an effective replacement for the isobutyl group in PMII. Finally, based on modelling studies, we provide a rationale for the selectivity of **1** and **2** for PMII versus PMIV and human cathepsin D.[18]

Results and Discussion

Enzyme inhibition

The inhibitory activity (IC_{50}) of pepstatin A against PMII, PMIV and the human enzymes cathepsin D and E was determined by using FRET-based proteinase assays. As previously reported,[15a] pepstatin A potently inhibited all four of these enzymes, with IC_{50} values at subnanomolar concentrations (Table 1). Fluorinated analogues of pepstatin A (**1** and **2**) also inhibited PMII very potently. The methyl ester **2** exhibited an IC_{50} of 3.7 ± 3 nM against PMII, and the acid form **1** displayed an IC_{50} of 6.4 ± 2 nM (mean $\pm$ standard deviation; number of experiments (*n*) is 4 in both instances). Both of these IC_{50} values were about ten-fold higher than the apparent IC_{50} of pepstatin A against the same enzyme (Table 1). These results indicate that, in this specific case, the isobutyl side chains of statine in pepstatin A can be replaced by Tfm without significantly loosing the biological activity of the inhibitor. It is known that the isobutyl of the statine side chains play a key role in PMII binding, particularly the central statine, which reaches into the S_1 position.[15] Therefore, we hypothesized that the central Tfm occupies the S_1 position in a similar manner to isobutyl; this would give rise to favourable interactions with the enzyme.

Table 1. Inhibitory activity of pepstatin A and its fluorinated variants (**1**–**7**) against aspartic proteinases. Inhibitory activity was determined by using FRET-based proteinase assays and is expressed as IC_{50} [nM] means $\pm$ standard deviation.

Compound	PMII	PMIV	Cathepsin D	Cathepsin E
pepstatin A	0.44 ± 0.023[a]	0.61 ± 0.11	0.64 ± 0.13	0.34 ± 0.16
1	6.4 ± 1.6	100 ± 16	620 ± 112	95 ± 54
2	3.7 ± 3.2	23 ± 7	730 ± 212	53 ± 13
3	>10000	>10000	>10000	>10000
4	8830	>10000	>10000	>10000
5	>10000	>10000	>10000	>10000
6	>10000	>10000	>10000	>10000
7	3200 ± 1200[b]	>10000	>10000	>10000

Four experiments were performed, except in cases [a] (eight) and [b] (three).

In order to assess the effect of fluorination on the selectivity of the inhibitors, the IC_{50} values of Tfm–pepstatins **1** and **2** were also determined against PMIV, cathepsin D and E. The methyl ester **2** and the acid **1** were 50–280-fold less active than pepstatin A against PMIV and cathepsin E (Table 1). The IC_{50} values for both compounds against cathepsin D were about 1000-fold higher than for pepstatin A. These results show that the substitution of the isobutyl side chains of pep-

statin A with Tfm has a more profound effect on the inhibitory activity against cathepsin D, cathepsin E and PMIV than against PMII. Furthermore, cathepsin D is more affected than PMIV and cathepsin E. This enzyme-dependent effect on the inhibitory potency of the modified compounds brings about a strong, and in this case desirable, enhancement of selectivity in favour of PMII versus the human cathepsins and PMIV. This finding indicates that replacement of isobutyl by Tfm can be used to fine-tune the activity of an inhibitor against one particular drug target, which potentially reduces the risk of side effects in patients.[19]

Shorter, N-terminally truncated Tfm variants of pepstatin A (**3**–**7**; Scheme 2) were also tested in the proteinase assays. These compounds proved to be inactive in all experiments performed; this confirms that the P_2–P_4 regions of pepstatin A are crucial for binding to aspartic proteinases.[15]

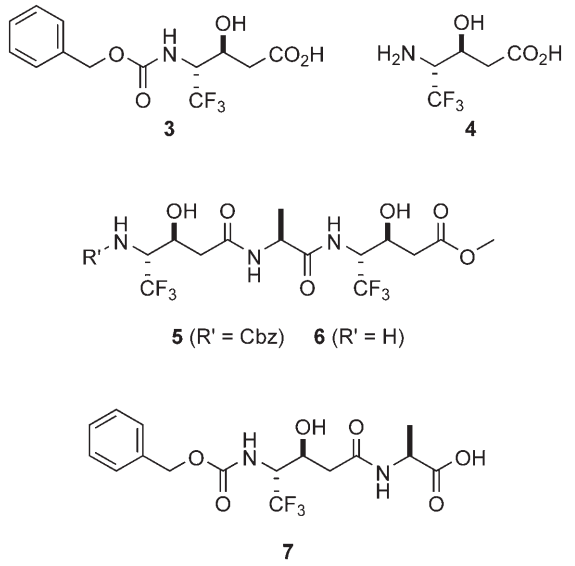

Scheme 2. Truncated forms of Tfm–pepstatin A tested in this study; Cbz = benzyloxycarbonyl.

Antiparasitic effects in vitro

The antiparasitic potency of pepstatin A has been reported to be weak in an in vitro proliferation test with *P. falciparum* in human red blood cells.[20] A possible explanation for this finding is that the peptidic pepstatin A molecule cannot easily penetrate the multiple layers of membranes that separate the target enzymes from the culture medium. In order to find out whether the fluorine side chains improve the antimalarial properties of pepstatin A, the Tfm variants **1**–**7** (Scheme 2) were tested against *P. falciparum* in red blood cell assays and compared to the effect of pepstatin A. As reported, pepstatin A inhibited the proliferation of *P. falciparum* in this assay with an IC_{50} concentration of 9.4 μM. However, all of the Tfm-substituted compounds where inactive at a concentration of 10 μM (data not shown). These results indicate that incorporation of fluorine had no beneficial effects on the bioactivity of pepstatin analogues in this experimental system.

Crystal structures of 1, 2 and pepstatin A bound to PMII

In order to gain a deeper insight into the binding mode of bis-Tfm–pepstatins and to assess the actual role of the Tfm groups in the binding process, we carried out an X-ray crystallographic study with **1** and **2** bound to PMII. For the sake of comparison, the crystal structure of the complex of pepstatin A with PMII was also reinvestigated and solved at a higher resolution than that available in the PDB.[15a] A summary of data processing and refinement is given in Table 2.

Table 2. Crystallographic data processing and refinement of the PMII complexes.

Parameter	Complex with		
	pepstatin A	**2**	**1**
space group	$P3_121$	$P3_121$	$P3_121$
cell constants [Å] *a*	141.11	141.65	141.18
b	141.11	141.65	141.18
c	7.10	98.35	97.38
resolution range	35–1.7	57–2.4	57–2.8
unique observations	122177	45644	27929
multiplicity	5.5	3.5	3.9
completeness [%]	99	95.5	95.5
R_{merge} [%]	9	9.5	11.9
number of atoms	5446	5544	5347
used reflections	122156	45617	27922
deviation bond length [Å]	0.008	0.010	0.012
deviation bond angles [°]	1.276	1.366	1.514
R_{fac}	0.214	0.20	0.216
free R_{fac}	0.237	0.258	0.268

Suitable crystals of inhibitor–PMII complexes were obtained in the presence of ammonium sulfate at pH 5.5–6.5, as described in the literature.[15a] All three PMII complexes crystallised in the same space group and comprised two enzyme molecules in the asymmetric unit, chains A and B. Comparison of chains A and B of each space group revealed significant differences between these two chains in all three structures. These differences are caused by crystal packing and were previously observed and discussed elsewhere.[15a,b] On the other hand, comparison of the individual A or B chains between the three complexes revealed very high similarity within both classes. The almost identical 3D structures of the inhibitor–PMII complexes indicate that pepstatin A and its Tfm-modified versions (**1** and **2**) bind to PMII in a very similar manner.

Both fluorinated inhibitors showed similar, single digit, nanomolar IC_{50} values against PMII (Table 1). In accordance with the IC_{50} values for **1** and **2**, the C-terminal carboxylate group was not found to significantly interact with PMII in any of the structures. It is worth noting that the Tfm group of the second modified-statine moiety was also not found to interact with PMII.

Comparison of PMII complexes with pepstatin A and its Tfm analogues

Despite the very high overall similarity between the three structures, small but significant differences were identified be-

tween the PM II complex with pepstatin A and the Tfm-modified pepstatins **1** and **2** (Figure 1). The most significant difference was noticed in the active site of chain B. The χ1 and χ2 angles of Phe111 were slightly changed. This difference in χ1 and χ2 angles resulted in a relocation of the Phe111 side chain

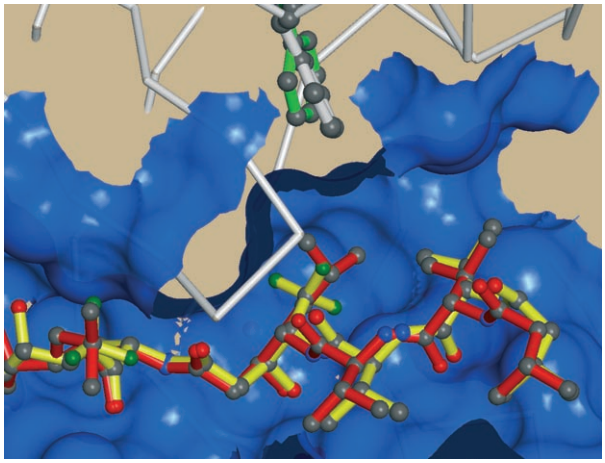

Figure 1. Superimposed X-ray structures of pepstatin A (red) and **2** (yellow) complexed to PM II (Cα representation) are shown against the active-site surface of PM II (blue). Due to very minor differences between the two structures, only one backbone (structure with compound **2**, white) is shown. A minor, but notable difference in side-chain conformation was identified with Phe111 (top middle) of the complex with **2** (grey).

towards the Tfm group of the inhibitors, thereby reducing the size of the S_1 pocket (Figure 2 A). In the A chains, a small variation in χ2 of Phe111 was also noticeable in the structures complexed to **1** and **2**. It appeared that PM II adapted to the Tfm group in the S_1 pocket by moving the side chain of the hydrophobic residue, Phe111, into this pocket and closer to the Tfm. This shift preserved the hydrophobic environment in the S_1 pocket and maintained the close interactions with the inhibitor side chain. On the other hand, the surface area of hydrophobic interactions between the enzyme and the Tfm side chain appeared to be reduced compared to the statine isobutyl. This "adaptive cavitation" should result in a lower binding energy and therefore reduced affinity of the inhibitor for the enzyme, as observed experimentally (Table 1). The S_1 pocket of PM II is formed by Ile32, Tyr77, Phe111, Ile123 and Gly216. These amino acids provide a purely hydrophobic environment for the S_1 pocket, which offers essentially no partners for polar interactions or hydrogen bonding with the Tfm group. The carbonyl of Gly216 was hydrogen bonded to a nitrogen atom from the inhibitor, and the aromatic rings of Tyr77 and Phe111 were not in an orientation that allowed interaction between their π electrons. Therefore, bipolar hydrophobic effects that are described to contribute to the binding energy of other fluorinated molecules[7b] are unlikely to affect the interaction of the S_1 pocket with the Tfm side chain in PM II.

Another difference was found in a loop that is formed between Asp10 and Met15 in chain A. The backbone conformation of this loop in the **1**–PM II and **2**–PM II complexes was very similar and was significantly different from that found in the pepstatin A complex. Indeed, **1** and **2** were located more deeply inside the S_3 pocket of PM II than pepstatin A. Such differences were not apparent in the B chains neither for the protein nor for the inhibitor. It is thus likely, that this region of the protein is influenced by crystal contacts. Furthermore, the loop between Asp10 and Met15 was not in contact with the Tfm or the isobutyl side chains of the pepstatin A variants. The experimental evidence led us to the conclusion that differences between the A chains of Tfm and isobutyl containing variants of pepstatin A did not represent the physiological situation of the complexes in solution, and that they were unlikely to be relevant for the present study. We conclude that the approximately tenfold loss of inhibitory activity for **1** and **2** towards PM II, compared to pepstatin A, is essentially due to the unfavourable "adaptive cavitation" that is created by the smaller Tfm group.

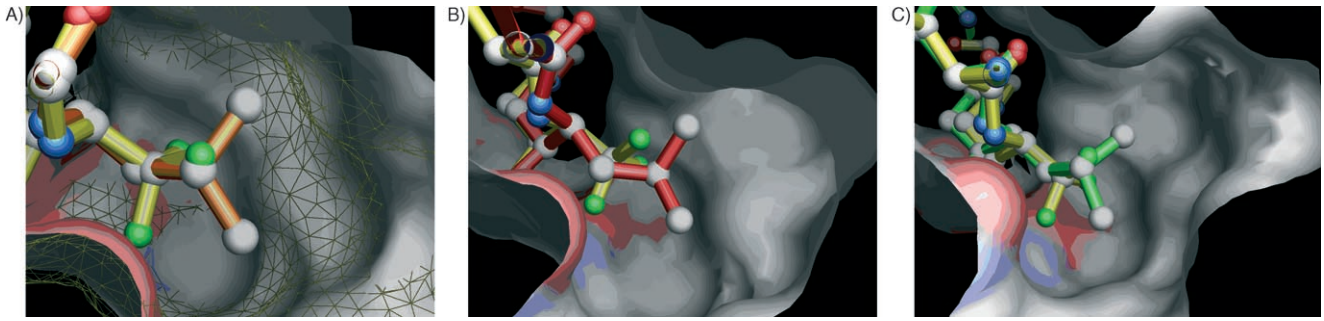

Figure 2. A) Superimposed X-ray structures of PM II complexed with pepstatin A (orange), and **2** (yellow). The view is a close up of the S_1 pockets. The electrostatic potential of the pepstatin A complex is depicted on the solid surface. The surface of the complex with **2** is shown as a mesh, which is not visible when hidden behind the surface. The relocation of Phe111 side chain in the complex with inhibitor **2** leads to an adaptation of the surface of the S_1 pocket. The corresponding protrusion is visible in the upper right corner of the figure. B) X-ray structure of PM VI complexed with pepstatin A (red) and superimposed with **2** (yellow) from the corresponding PM II structure. The electrostatic-potential surface of the pepstatin A complex is depicted. The viewing angle is analogous to that in A). The presence of Leu in PM IV at the position that corresponds to Phe111 in PM II (upper right of the figure) results in an enlarged cavity that cannot be adequately filled by the Tfm side chain. C) X-ray structure of cathepsin D complexed with pepstatin A (green) and superimposed with **2** (yellow) from the corresponding PM II structure. The superimposition was based on the active-site residues of the two proteins. The electrostatic-potential surface of the pepstatin A complex is depicted. The viewing angle is analogous to that in A). The presence of Val in cathepsin D at the position that corresponds to Ile32 in PM II (to the lower right side of the isopropyl side chain) leaves a cavity that cannot be adequately filled by the Tfm side chain.

Models of PMIV and cathepsin D complexed with Tfm–pepstatin A analogues

In order to understand the structural factors underlying the difference in inhibitory potency of **1** and **2** towards PMII, PMIV and cathepsin D, the 3D structures of PMIV and cathepsin D in complex with pepstatin A (PDB entry codes 1LS5[15b] and 1LYB[21]) were used to model structures for these enzymes complexed with the Tfm variants. A crystallographic structure was not available for cathepsin E, so this enzyme was not included in the analysis.

Due to the high sequence homology between PMII and PMIV, the enzymes were predicted to have very similar folds overall. This notion was confirmed upon comparison of pepstatin A complexed structures of these two enzymes. The high structural similarity included the active site where the very hydrophobic environments of the S_1 and S_3 pockets in PMII was conserved in PMIV. Amino acids Ile32, Asp34, Tyr77, Phe111, Ile123 and Gly216 pointed into the S_1 pocket of the PMII complexes and were located close to the Tfm group. Of these, Asp34, Tyr77, Ile123 and Gly216 are conserved in all aspartic proteinases discussed in this paper; these are therefore unlikely to be responsible for the differences observed in the IC_{50} values between these enzymes. Of the potentially critical residues Ile32 and Phe111, only the latter varies between PMII and PMIV (Leu in PM VI). With the smaller Leu residue the S_1 pocket in PMIV becomes bigger than in PMII (Figure 2B). Thus, it probably loses the ability to adapt to the Tfm group in a manner similar to PMII, without rearranging the protein backbone. Interactions between the inhibitors and enzymes outside the S_1 pocket could also be modelled for PMIV and no difference was observed when compared with PMII. Note that the Tfm group of the second modified statine moiety was not found to significantly interact with PMII and the same appeared to hold true for PMIV. Therefore, the presence of Tfm or isobutyl at this position was not expected to affect the binding affinity of pepstatin A or its variants for PMII or PMIV. The inability of the S_1 pocket of PMIV to adapt to a smaller ligand is thus a possible explanation for the loss of inhibitory potency of the Tfm variants against PMIV compared to PMII.

The affinity of **1** and **2** for cathepsin D was found to be about 1000-fold lower than that of pepstatin A, and the IC_{50} values of **1** and **2** were about two orders of magnitude lower for cathepsin D than for PMII. One possible contributor to this significant effect could be residue Val23 in cathepsin D. The equivalent residue in PMII and PMIV is Ile32 which points towards the inhibitor in the S_1 pocket, as outlined above. Based on the pepstatin A costructure, Val23 leads to an enlargement of the S_1 pocket in cathepsin D compared to PMII, where the corresponding position is occupied by the larger Ile (Figure 2C). Therefore, the isobutyl side chain of pepstatin A, which points into the S_1 pocket of the structure, was unable to fill the available space completely and optimally. Without a conformational adaptation by the enzyme, this space would be filled even less adequately with a Tfm side chain instead of the isopropyl. This is hypothesised to lead to a weaker interaction between cathepsin D and Tfm-modified pepstatin A compared to pepstatin A, and contributes to the lower affinity of the Tfm analogues. In addition, the proline-rich loop (residues 310–318) of cathepsin D is significantly longer and more rigid than the corresponding loop of PMII. In cathepsin D, the isobutyl side chain of the second statine moiety tightly interacted with the proline-rich loop. This interaction would be expected to contribute to the binding energy of pepstatin A in cathepsin D. In contrast, all of the three structures of PMII were completely devoid of such interactions. Due to the potential flexibility of the proline-rich loop in cathepsin D, it was not possible to predict whether similar interactions would affect the binding of the isobutyl and Tfm side chains. However, a lack of interactions between the second Tfm and the proline-rich loop in cathepsin D would contribute to the observed shift in IC_{50} values.

Conclusion

Replacement of the two isobutyl side chains of pepstatin A with Tfm groups has produced a bis-Tfm analogue **1**, and its methyl ester **2**. These two compounds retained nanomolar inhibitory potency against the protozoal aspartic proteinase, PMII. This suggests that the Tfm group can be used as an effective backbone substituent in this case. Consistent with this assumption, the crystal structures of the three complexes of **1**, **2** and pepstatin A with PMII showed only small differences to each other. Detailed analysis of the PMII complexes showed that Phe111 has a critical role in the interaction with the P_1 side chain of pepstatin A or its Tfm analogues. The second isobutyl (or Tfm) side chain did not interact with PMII, neither did the carboxy termini of pepstatin A and its variants. This is consistent with the similar IC_{50} values observed for **1** and **2** against PMII.

Replacement of the isobutyl side chains of pepstatin A with Tfm had different effects on the inhibitory activity of the compounds against PMII, PMIV and the human cathepsins D and E. In fact, a significant shift in selectivity was observed for **1** and **2** in favour of PMII. Comparison of the three crystal structures of PMII presented here, with the X-ray structures of PMIV and cathepsin D complexed to pepstatin A, allowed a rationalisation of the different inhibition profiles against these enzymes. The interaction of Tfm with those amino acids that point into the highly conserved and purely hydrophobic S_1 pockets appeared to be critical for inhibitory activity. In particular, amino acids corresponding to Phe111 and Ile32 in PMII were found to play key roles in this context.

The results and observations presented here offer useful clues to medicinal chemists for the design of fluorinated analogues of bioactive molecules. Due to the extraordinary properties of fluorine, the use of fluorinated analogues can help to change affinity and selectivity profiles of lead compounds during drug discovery, and is expected to influence other properties relevant for clinical development of compounds.

Experimental Section

Chemistry: Fluorinated peptidomimetics **1**–**7** were synthesised as described in the literature.[9]

Protein expression: PMII and IV were produced in *E. coli* as described in the literature.[22] DNA encoding the last 48 residues of the pro region and the whole, mature sequence of *P. falciparum* PMII were cloned into the T7-dependent expression vector pET3a (clone obtained from C. Berry, Cardiff School of Biosciences, Cardiff University, Cardiff, Wales, UK). Protein was expressed in *E. coli* BL21 (DE3) as inclusion bodies, solubilised and refolded as described by Hill et al.[22] The resulting soluble, refolded protein was purified by using a ligand-affinity column followed by size-exclusion chromatography in Na or K phosphate (20 mM, 100 mM NaCl, pH 6.5) and was concentrated for crystallisation by using an Amicon Ultra-centrifugal concentrator.

Inhibition tests: Proteolytic activities of PMII, PMIV, cathepsin D (Athens Research, Athens, GA, USA; no. 16–12–030104) and cathepsin E[23] were determined by using FRET-based assays with a substrate purchased from Bachem (M-2120). Enzyme (1 nM) was incubated with the substrate (1 μM) at 37 °C in sodium acetate (50 mM, pH 5), glycerol (12.5%, *w/v*), BSA (0.1%, *w/v*) and DMSO (10%). Enzyme activity was derived from the turnover rate of the substrate and was monitored by the increase in fluorescent signal over time. Fluorescence was determined with a FluoroStar Galaxy (BMG Lab Technologies, Inc., Offenburg, Germany) by using 355 and 520 nm excitation and emission filters, respectively. Test compounds were dissolved and diluted in DMSO (100%). Inhibitory activity of the compounds is expressed as IC_{50}, which represents the concentration of compound that inhibits 50% of the maximal (uninhibited) enzyme activity.

X-ray crystallography: Crystals were obtained with ammonium sulfate (pH 5.5–6.5) as described.[15a] Data were collected at the PX beamline at the Swiss Light Source (Paul Scherrer Institute, Villigen, Switzerland). Data processing, structure solution and refinement were carried out with programs from the CCP4-program package.[24] For manual rebuilding of the structure, the program Moloc was used (www.moloc.ch). Summary of the data processing and refinement is given in Table 2.

Crystallographic data for the complexes of **1**, **2** or pepstatin A with PMII have been deposited with the PDB (http://pdbbeta.rcsb.org; ID codes 1XE6, 1XE5 and 1XDH respectively).

Acknowledgements

We would like to thank Antoinette Amrein, Alain Chambovey, Karsten Kropp and Adrian Roth for skilful experimental support, Dr. Daniel Bur for support with modelling and very helpful discussions, and Dr. Clemens Schulze-Briese, Takashi Tomizaki and their group for their support in setting up the beamline. We are indebted to Dr. Reto Brun and Christian Scheurer for performing antimalarial tests in red blood cells. We also thank MIUR (Cofin 2002, Project "Peptidi Sintetici Bioattivi"), Politecnico di Milano and C.N.R. for economic support.

Keywords: fluorine · inhibitors · peptidomimetics · protein structures · X-ray diffraction

[1] R. E. Banks, J. C. Tatlow, B. E. Smart, *Organofluorine Chemistry: Principles and Commercial Applications*, Plenum, New York, **1994**, pp. 537–538.
[2] M. Charton, *J. Am. Chem. Soc.* **1975**, *97*, 1552–1556.
[3] B. E. Smart, *J. Fluorine Chem.* **2001**, *109*, 3–11.
[4] F. Leroux, *ChemBioChem* **2004**, *5*, 644–649.
[5] K. Mikami, Y. Itoh, M. Yamanaka, *Chem. Rev.* **2004**, *104*, 1–16.
[6] For recent reviews of the topic: a) J. C. Biffinger, H. W. Kim, S. G. DiMagno, *ChemBioChem* **2004**, *5*, 622–627; b) F. M. D. Ismail, *J. Fluorine Chem.* **2002**, *118*, 27–33.
[7] a) J. A. Olsen, D. W. Banner, P. Seiler, B. Wagner, T. Tschopp, U. Obst-Sander, M. Kansy, K. Müller, F. Diederich, *ChemBioChem* **2004**, *5*, 666–675, and references therein; b) R. Paulini, K. Müller, F. Diederich, *Angew. Chem.* **2005**, *117*, 1820–1839; *Angew. Chem. Int. Ed.* **2005**, *44*, 1788–1805.
[8] H.-J. Böhm, D. Banner, S. Bendels, M. Kansy, B. Kuhn, K. Müller, U. Obst-Sander, M. Stahl, *ChemBioChem* **2004**, *5*, 637–643, and references therein.
[9] a) P. Bravo, E. Corradi, C. Pesenti, B. Vergani, F. Viani, A. Volonterio, M. Zanda, *Tetrahedron: Asymmetry* **1998**, *9*, 3731–3735; b) C. Pesenti, A. Arnone, S. Bellosta, P. Bravo, M. Canavesi, E. Corradi, M. Frigerio, S. V. Meille, M. Monetti, W. Panzeri, F. Viani, R. Venturini, M. Zanda, *Tetrahedron* **2001**, *57*, 6511–6522.
[10] H. Umezawa, T. Aoyagi, H. Morishima, M. Matsuzaki, M. Hamada, T. Takeuchi, *J. Antibiot.* **1970**, *23*, 259–262.
[11] For a recent review on aspartic proteases (also called peptidases): B. M. Dunn, *Chem. Rev.* **2002**, *102*, 4431–4458.
[12] R. Banerjee, J. Liu, W. Beatty, L. Pelosof, M. Klemba, D. Goldberg, *Proc. Natl. Acad. Sci. USA* **2002**, *99*, 990–995.
[13] a) C. Boss, S. Richard-Bildstein, T. Weller, W. Fischli, S. Meyer, C. Binkert, *Curr. Med. Chem.* **2003**, *10*, 883–907, and references therein; b) J. Wiesner, R. Ortmann, H. Jomaa, M. Schlitzer, *Angew. Chem.* **2003**, *115*, 5432–5451; *Angew. Chem. Int. Ed.* **2003**, *42*, 5274–5293.
[14] G. H. Coombs, D. E. Goldberg, M. Klemba, C. Berry, J. Kay, J. C. Mottram, *Trends Parasitol.* **2001**, *17*, 532–537.
[15] a) A. M. Silva, A. Y. Lee, S. V. Gulnik, P. Majer, J. Collins, T. N. Bhat, P. J. Collins, R. E. Cachau, K. E. Luker, I. Y. Gluzman, S. E. Francis, A. Oksman, D. E. Goldberg, J. W. Erickson, *Proc. Natl. Acad. Sci. USA* **1996**, *93*, 10034–10039; b) O. A. Asojo, S. V. Gulnik, E. Afonina, B. Yu, J. A. Ellman, T. S. Haque, A. M. Silva, *J. Mol. Biol.* **2003**, *327*, 173–181. For extensive work on pepstatin A analogues as inhibitors of aspartic proteinases, see: c) M. G. Bursavich, D. H. Rich, *J. Med. Chem.* **2002**, *45*, 541–558; d) D. H. Rich, *J. Med. Chem.* **1985**, *28*, 263–273.
[16] For the standard nomenclature of substrate residues and their corresponding binding sites on the enzyme, see: R. E. Babine, L. E. Bender, *Chem. Rev.* **1997**, *97*, 1359–1472.
[17] For some examples of statine-based peptidomimetics as Plasmepsins inhibitors: a) A. Dahlgren, I. Kvarnström, L. Vrang, E. Hamelink, A. Hallberg, Å. Rosenquist, B. Samuelsson, *Bioorg. Med. Chem.* **2003**, *11*, 827–841; b) T. S. Haque, A. G. Skillman, C. E. Lee, H. Habashita, I. Y. Gluzman, T. J. A. Ewing, D. E. Goldberg, I. D. Kuntz, J. A. Ellman, *J. Med. Chem.* **1999**, *42*, 1428–1440; c) C. D. Carroll, T. O. Johnson, S. Tao, G. Lauri, M. Orlowski, I. Y. Gluzman, D. E. Goldberg, R. E. Dolle, *Bioorg. Med. Chem. Lett.* **1998**, *8*, 3203–3206.
[18] For recent examples of nanomolar peptidomimetic inhibitors of plasmepsins that spare cathepsin D: a) P.-O. Johansson, Y. Chen, A. K. Belfrage, M. J. Blackman, I. Kvarnström, K. Jansson, L. Vrang, E. Hamelink, A. Hallberg, Å. Rosenquist, B. Samuelsson, *J. Med. Chem.* **2004**, *47*, 3353–3366; b) K. Ersmark, I. Feierberg, S. Bjelic, E. Hamelink, F. Hackett, M. J. Blackman, J. Hultén, B. Samuelsson, J. Åqvist, A. Hallberg, *J. Med. Chem.* **2004**, *47*, 110–122, and references therein.
[19] For a review on aspartic-peptidase inhibitors and their implications in drug development, see: C. Dash, A. Kulkarni, B. Dunn, M. Rao, *Crit. Rev. Biochem. Mol. Biol.* **2003**, *38*, 89–119.
[20] P. J. Rosenthal, *Exp. Parasitol.* **1995**, *80*, 272–281.
[21] E. T. Baldwin, T. N. Bhat, S. Gulnik, M. V. Hosur, R. C. Sowder II, R. E. Cachau, J. Collins, A. M. Silva, J. W. Erickson, *Proc. Natl. Acad. Sci. USA* **1993**, *90*, 6796-6800
[22] a) J. Hill, L. Tyas, L. H. Phylip, J. Kay, B. M. Dunn, C. Berry, *FEBS Lett.* **1994**, *352*, 155–158; b) D. M. Wyatt, C. Berry, *FEBS Lett.* **2002**, *513*, 159–162.
[23] J. Hill, D. S. Montgomery, J. Kay, *FEBS Lett.* **1993**, *326*, 101–104.
[24] Collaborative Computational Project, Number 4, *Acta Crystallogr. D Biol. Crystallogr.* **1994**, *50*, 760–763.

Received: April 27, 2005
Revised: August 22, 2005
Published online on November 24, 2005

